The effect of surface charge balance on thermodynamic stability and kinetics of refolding of firefly luciferase

Khosrow Khalifeh, Bijan Ranjbar, Bagher Said Alipour & Saman Hosseinkhani**

Department of Biophysics & Biochemistry, Faculty of Biological Sciences, Tarbiat Modares University, P.O. Box, 14115-175 Tehran, Iran

Thermodynamic stability and refolding kinetics of firefly luciferase and three representative mutants with depletion of negative charge on a flexible loop via substitution of Glu by Arg (ER mutant) or Lys (EK mutant) as well as insertion of another Arg in ER mutants (ERR mutant) was investigated. According to thermodynamic studies, structural stability of ERR and ER mutants are enhanced compared to WT protein, whereas, these mutants become prone to aggregation at higher temperatures. Accordingly, it was concluded that enhanced structural stability of mutants depends on more compactness of folded state, whereas aggregation at higher temperatures in mutants is due to weakening of intermolecular repulsive electrostatic interactions and increase of intermolecular hydrophobic interactions. Kinetic results indicate that early events of protein folding are accelerated in mutants. [BMB reports 2011; 44(2): 102-106]

INTRODUCTION

It has been suggested that electrostatic interactions and surface charges play critical role in the folding kinetics and equilibrium stability of proteins (1-3). Garcia-Mira *et al.* (4) had performed comparative folding experiments with protein engineering strategies and found that long-range columbic interactions are important for organizing and stabilizing native-like structure in the early stage of protein folding. Moreover, it was shown that surface charges have important effects on the stability of a variant of protein G B1 domain and such effects are not eliminated by salt screening (5).

However, there are suggestions on destabilizing effects of charged and polar groups (6, 7); whereas some results indicate that surface charge-charge interactions are not essential for protein folding and stability (8).

Luciferases are enzymes in bioluminescence organisms that

*Corresponding author. Tel: +989123840600; Fax: +982188007598; E-mail: ranjbarb@modares.ac.ir, saman_h@modares.ac.ir

produce light from conversion of chemical energy into an excited electronic state which results in emission of photon in the visible region. The bioluminescence color of fireflies varies from green to red. It has been shown that only the railroad worm luciferase *Phrixothrix hirtus* can naturally emit red light. In order to elucidate the mechanisms of the bioluminescence color change, extensive studies were carried out and several mechanisms have been proposed (9, 10). Multiple sequence alignment of primary structure of *Phrixothrix hirtus* showed a missed Arg^{353} in a flexible loop in green emitter fireflies. Accordingly, site directed mutagenesis technique were used for insertion of Arg in the corresponding position in the loop of firefly luciferase *Lampyris turkestanicus* (11) and it was shown that Arg^{353} plays a critical role in the bioluminescence color (12). A similar study on the North American firefly luciferase *Photinus pyralis* indicated that the presence of positive charges on the same loop has significant effects on the emitted light shift from green to red (13).

Here, we investigated the refolding kinetics and thermodynamic stability of native and mutants of firefly luciferase (*Lampyris turkestanicus*, Accession No. AAU85360); where the surface charges of strands connecting loop were modified using site directed mutagenesis. It was shown that positive charge saturation on this flexible loop results in the change of color emission in firefly luciferase (14).

RESULTS AND DISCUSSION

In order to elucidate the relationships between structural properties and color emission of bioluminescence, thermodynamic stability and kinetics of refolding of firefly luciferase and its mutants were investigated.

The structures of WT and mutant luciferases are modeled with Swiss Model Program (15-17), which shows high structural homology with *Photinus pyralis* firefly luciferase (18).

Supplementary data 1 shows a part of protein containing β-strands connecting loop as well as a brief description of its sequence and mutations. It can be seen that a residue with negatively-R group (Glu) has been replaced by positively-R group (Arg and Lys) near two successive Asp to give ER, ERR and EK mutants. This loop is located between the 15th and 16th β-strands at N-terminal domain.

Fig. 1 shows the normalized urea denaturation curves for

WT and mutant proteins monitored by fluorescence spectroscopy.

The equilibrium denaturation parameters of WT and mutant forms are listed in Table 1. According to thermodynamic data (Table 1), higher stability of ER and ERR mutants is a consequence of larger values of both $m_{U\text{-}N}$ and $[Urea]_{50\%}$. The thermodynamic values of $m_{U\text{-}N}$ shows the solvent accessibility of state U with respect to state N. Therefore, increase of m-value in mutants may be related to more compactness of folded state or lower level of residual structure in the unfolded state as well as increasing protein size through insertion of a bulkier side-chain of Arg, especially in ERR mutant (19). It is worthy to mention that while $[Urea]_{50\%}$ of EK mutant is lower than that of WT protein; the mutant shows a higher m-value. Therefore, its free energy of unfolding in water is approximately the same as WT.

A typical kinetic trace of refolding of WT protein is shown in supplementary data 2. These traces were fitted to double exponential function to get rate constants of refolding and unfolding. However; in this study the major phases were used to generate chevron plots and the minor phases are not analyzed further.

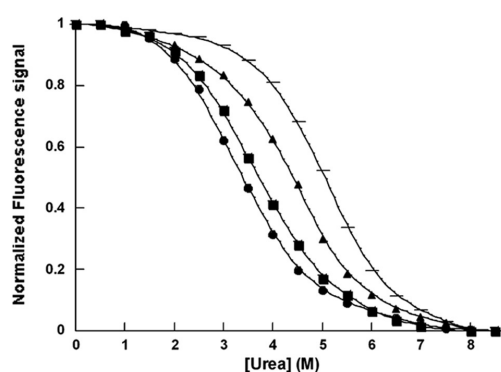Fig. 2 shows chevron plots of WT and mutant proteins as the logarithms of rate constants for folding and unfolding versus urea concentrations. As shown in Fig. 2; a linear dependence between unfolding arm of log k_u and urea concentrations was observed. Whereas, the refolding limb of plots of log k_f versus [Urea] shows downward curvatures, indicating of a folding intermediate accumulating at low urea concentrations (20). Hence, data from chevron plots were best fitted into equation 4 and the kinetic parameters of WT and mutant proteins are shown in Table 1.

Considering the kinetic data (Table 1) early events of protein folding, conversion of unfolded to intermediate state, was accelerated in the mutants. This step is followed by conversion of intermediate to final folded state via rate limiting transition state.

The energy levels of intermediate, transition and folded state are shown in Fig. 3 as difference free energy diagram. It should be noted that by taking unfolded state as reference, the experimentally measured energy differences vary from the true energy differences. This is due to neglecting of the energy differences of unfolded state between WT and mutant proteins which does not affect the qualitative interpretation of the results (21).

According to chevron plots, the appearance of kinetic intermediate at low urea concentration might indicate that the
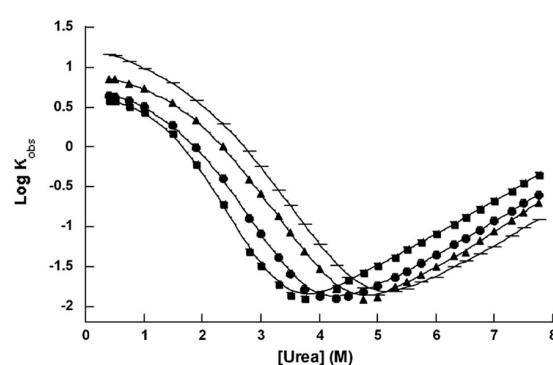

Fig. 1. Normalized equilibrium denaturation curves of the wild type and mutant proteins, [WT (■), ER (▲), ERR (—) and EK (●)]. Solid line represents the fitting of experimental data to equation 1 assuming equilibrium two state model.

Fig. 2. Chevron plots. Denaturant dependence of log k_{obs} of folding and unfolding kinetics of WT (■), ER (▲), ERR (—) and EK (●). The solid line represents the best fit of kinetics data to equation 4.

Table 1. Thermodynamic and Kinetic parameters of WT and mutant proteins

	Thermodynamic parameters[a]			Kinetic parameters[b]		
	$[Urea]_{50\%}$	$m_{U\text{-}N}$	$\Delta G_{U\text{-}N}^{H_2O}$	$K_{UI}^{H_2O}$	$K_{IN}^{H_2O}$	$K_{NI}^{H_2O}$
WT	3.58 ± 0.03	0.72 ± 0.03	2.58 ± 0.12	216 ± 50	13 ± 2	0.67 ± 0.04
EK	3.11 ± 0.04	0.80 ± 0.03	2.49 ± 0.12	226 ± 52	23 ± 2	0.78 ± 0.03
ER	4.48 ± 0.05	0.91 ± 0.05	4.08 ± 0.26	397 ± 116	51 ± 7	1.02 ± 0.03
ERR	5.04 ± 0.03	0.94 ± 0.03	4.74 ± 0.18	495 ± 122	52 ± 6	1.35 ± 0.02

[a]Obtained from Urea denaturation experiments by fitting experimental data of Fig. 1 to equation 1. $[Urea]_{50\%}$ is in M, m-value in $Kcalmol^{-1}M^{-1}$ and energy in $Kcalmol^{-1}$, [b]Obtained from fitting of experimental kinetic data of Fig. 2 to equation 4. Rate constants are in S^{-1}
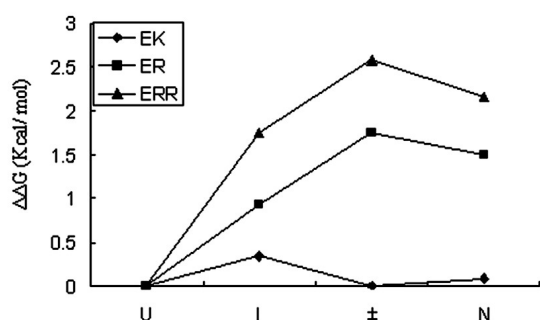
Fig. 3. Diagram of free energy changes of structural elements in refolding pathway between WT and mutant proteins. The absolute values of free energy changes were used for plotting the difference energy diagram. Free energies of intermediate and transition states are acquired from kinetic studies and that for folded state from equilibrium denaturation experiments. The free energies are normalized by taking the unfolded state as reference.

structure of intermediate is more similar to the native state than unfolded one. Based on kinetic data in Table 1, the first step of folding reaction is related to early events of protein folding which result in formation of an intermediate state. Moreover, all mutants have larger rate constants than WT protein; indicating faster folding in the early stage for mutants compared to WT protein. On the other hand, this loop plays an active role in early events of protein folding and its closure is essential for facilitating the condensation of β-strands. This may be due to higher closure propensity of loop upon mutation which mediated via attractive electrostatic and hydrophobic interactions, so that unfavorable chain entropy is relatively offset during folding. As a plausible explanation, interactions between the charge residues may be in short and long ranges and such interactions can involve multiple charge residues. This is because that during protein folding, short range interactions can exist after chain immobilization, being independent of chain entropy; whereas, long range electrostatic interactions are essential for lowering the chain entropy by gaining the enthalpic interactions (4).

Consistent with the above mentioned observations, the assessments of protein aggregation at higher temperatures upon heat-induced aggregation were carried out (Supplementary data 3) and it was shown that aggregation started at approximately 41°C for WT and 39, 38 and 35°C for EK, ER and ERR respectively. On the other hand, upon deletion of negative side chain of protein; it becomes prone to aggregation. This phenomenon is apparently in contrast with the stability of the proteins measured at lower temperatures by chemical denaturation studies (Table 1). It seems that this contradiction is originated from unusual properties of hydrophobic interaction which is temperature dependent and increases in magnitude with increasing temperature, whereas other types of interactions such as electrostatic decrease in strength as temperature increases (22, 23). In the case of aggregation, it seems

clear that there is a competition between intermolecular attractive hydrophobic interactions and that of repulsive electrostatic interaction so that increasing the temperature tend to strengthens the former while the latter being weakened. Therefore, the repulsive electrostatic interactions between two approaching proteins upon conditions that increase molecular collision are diminished and the probability of aggregation at higher temperatures is increased. It also appears that substitution of negative side chain of Glu by positive side chain of Arg, in the vicinity of two Asp results in further neutralization of negative charge of loop and the presence of bulkier hydrophobic side chain of Arg in ERR and ER mutants is also a key factor in promotion of aggregation at higher temperature due to increasing the strength of hydrophobic interaction at higher temperatures.

Overall, comparing the involving residues of ER and ERR mutants show that ERR has more positive charge as well as hydrophobic contact surface area than that of ER and EK. Generally speaking, these structural differences have two important consequences; first, it is related to lower affinity of positive charge of Arg and Lys to water molecules compared to the negative side chain of Glu (24, 25). Second, the bulkier hydrophobic side chain of Arg induces unfavorable interaction with polar solvent during the unfolding and more favorable interactions during the folding process. Accordingly, it can be suggested that Vander Waals, hydrophobic and electrostatic interactions as short range interactions in ER and ERR mutants are dominant factors in determining the stability of intermediate and folded states. Such short range interactions can lower the entropy of loop in the intermediate and folded state.

MATERIALS AND METHODS

Protein expression and purification
Protein expression and purification were carried out as described previously (14).

Stability measurements
Urea-induced unfolding of proteins was followed by fluorescence Spectroscopy. The buffer used for equilibrium denaturation was 50 mM Tris, pH7.8 and 25°C.

First, buffered stock solutions of Urea were prepared (0 M and 8.5 M) in 50 mM Tris, pH 7.8. After filtering, the buffered stock solutions were mixed in appropriate proportions to give final denaturant concentration ranging from 0 to 8.5 M with final protein concentration of 20 μM. Fluorescence measurements were performed using BioLogic Mos-250 Spectrophotometer. Excitation was at 290 nm and emission spectra were recorded between 300-400 nm at a rate of 60 nm per minute (Excitation and emission slits were set to 5 nm).

The equilibrium curves were fitted using Kaliedagraph analysis software by equation 1, assuming a two state model (26, 27):

$$F_{335} = \{(\alpha_N + \beta_N[Urea]) + (\alpha_U = \beta_U[Urea])\} \times \exp((m_{U-N}([Urea]$$

$$-[Urea]_{50\%}))/RT)/\{1+\exp((m_{U-N}([Urea]-[Urea]_{50\%}))/RT) \qquad (1)$$

Where F_{335} is the fluorescence intensity at 335 nm at a given concentration of urea [Urea], α_N and α_U are intercepts, and β_N and β_U are the slopes of the baselines. $[Urea]_{50\%}$ is the concentration of urea at which half of the protein is denatured, R is the gas constant and T is the temperature in Kelvin. m_{U-N} is a constant which is proportional to increase in the solvent accessible surface area between native and denatured states (27).

The free energy of unfolding in the presence of urea, $\Delta G_{U-N}^{[Urea]}$ is related to the concentration of denaturants as equation 2:

$$\Delta G_{U-N}^{[Urea]} = \Delta G_{U-N}^{H_2O} - m_{U-N}([Urea] \qquad (2)$$

Accordingly, the free energy of unfolding in the absence of urea, $\Delta G_{U-N}^{H_2O}$ can be estimated as:

$$\Delta G_{U-N}^{H_2O} = m_{U-N}[Urea]_{50\%} \qquad (3)$$

Kinetics experiments

Kinetic measurements were carried out with a BioLogic μ-SFM-20 flourescence detected Stopped-flow using a 0.8 cm cuvette (FC-08). Data were collected and analyzed with the Biokin analysis software. Reaction progress of folding and unfolding was monitored by fluorescence signal (Excitation: 290 nm; emission: 335 nm).

The refolding reaction was initiated following 10 or 15 fold dilution of the protein unfolded in 50 mM Tris, pH 7.8, containing concentrated Urea, into 50 mM Tris, pH 7.8 containing different concentration of Urea ranging from 0 to 5 M.

Unfolding was initiated by mixing one volume of protein in 50 mM tris buffer, pH, 7.8 with 6 or 10 volume of Tris buffer containing different concentrations of urea.

Kinetic traces were fitted to double exponential function to get rate constants of refolding and unfolding and the major phases were used for further analysis. All kinetic measurements were carried out at 25°C.

Data from kinetic experiments as the logarithms of rate constants for refolding and unfolding versus Urea concentration (chevron plots) were fitted by kaliedagraph analysis software into equation 4 assuming a three state model and the presence of kinetic on-pathway intermediate (28):

$$\log k_{obs} = Log[\frac{k_{UI}^{H_2O}\exp(-m_{UI}[Urea]/RT)}{1+k_{UI}^{H_2O}\exp(-m_{UI}[Urea]/RT)}]\times \qquad (4)$$

$$k_{IN}^{H_2O}\exp(-m_{IN}^{\ddagger}[Urea]/RT)+k_{NI}^{H_2O}\exp(-m_{NI}^{\ddagger}[Urea]/RT)$$

Where, $k_{ij}^{H_2O}$ is the rate constant of conversion i to j extrapolated to water and m_{ij} is the difference in exposed surface area between i and j states. $m_{ij}^{\ddagger}$ refers to the m-values for the formation of transition state from i to j state.

The free energy of intermediate is calculated using the following thermodynamic equation:

$$\Delta G_{I-N} = -RT\ln\frac{k_{NI}}{k_{IN}} \qquad (5)$$

The free energy of transition state is calculated using the transition state theory and according to equation 6 (29):

$$k_{NI} = (\frac{K_BT}{h})\exp(\frac{-\Delta G_{IN}}{RT}) \qquad (6)$$

In calculating the energy levels of structural elements, all energy levels should be normalized by taking the unfolded state as reference (30).

Aggregation control

Heat-induced aggregation was followed by recording the increase in absorbance at 360 nm. Luciferases (Wild Type and Mutants) in 50 mM tris buffer, pH 7.8, and 10 μM concentration with total volume of 1 ml in closed cuvette were heated from 20 to 45°C in a Unicam UV/Vis spectrophotometer equipped with thermal circulator bath.

REFERENCES

1. Loladze, V. V., Ibarra-Molero, B., Sanchez-Ru, L. M. and Makhatadze, G. I. (1999) Engineering a thermostable protein via optimization of charge-charge interactions on the protein surface. *Biochemistry* **38**, 16419-16423.
2. Akk, M. and Forsen, S. (1990) Protein stability and electrostatic interactions between solvent-exposed charged side chains. *Proteins* **8**, 23-29.
3. Roca, M., Messer, B. and Warshel, A. (2007) Electrostatic contributions to protein stability and folding energy. *FEBS Lett.* **581**, 2065-2071.
4. Garcia-Mira, M. M. and Schmid, F. X. (2006) Key role of coulombic interactions for the folding transition state of the Cold Shock Protein. *J. Mol. Biol.* **364**, 458-468.
5. Lindman, S., Xue, W., Szczepankiewicz, O., Bauer, M. C., Nilsson, H. and Lins, S. (2006) Salting the charged surface: pH and salt dependence of protein G B1 stability. *Biophys. J.* **90**, 2911-2921.
6. Loladze, V. V. and Makhtadze, G. I. (2002) Removal of surface charge-charge interactions from ubiquitin leaves the protein folded and very stable. *Protein Sci.* **11**, 147-177.
7. Hendsch, Z. and Tidor, B. (1994) Do salt bridges stabilize proteins? A Continuum electrostatic analysis. *Protein Sci.* **3**, 211-226.
8. Katherine, L. G. (2005) Eliminating positively charged lysine ε-NH^{3+} Groups on the surface of carbonic anhydrase has no significant influence on its folding from Sodium Dodecyl Sulfate. *J. Am. Chem. Soc.* **127**, 4707- 4714.

9. Branchini, B. R., Southworth, T. L., Murtiashaw, M. H., Magyar, R. A., Gonzalez, S. A., Ruggiero, M. C. and Stroh, J. G. (2004) An Alternative Mechanism of Bioluminescence Color Determination in firefly luciferase. *Biochemistry* **43**, 7255-7262.

10. Tafreshi, N., Sadeghizadeh, M., Emamzadeh, R., Ranjbar, B., Naderi-Manesh, H. and Hosseinkhani, S. (2008) site-directed mutagenesis of firefly luciferase: Implication of conserved residue(s) in bioluminescence emission among firefly luciferases. *Biochem. J.* **412**, 27-33.

11. Alipour, B. S., Hosseinkhani, S., Nikkhah, M., Naderi-Manesh, H., Chaichi, M. J. and Osaloo, S. K. (2004) Molecular cloning, sequence analysis, and expression of a cDNA encoding the luciferase from the glow-worm *Lampyris turkestanicus*. *Biochem. Biophys. Res. Commun.* **325**, 215-222.

12. Tafreshi, N., Hosseinkhani, S., Sadeghizadeh, M., Sadeghi, M., Ranjbar, B. and Naderi-Manesh, H. (2007) The Influence of Insertion of a Critical Residue (Arg^{356}) in Structure and Bioluminescence Spectra of Firefly Luciferase. *J. Biol. Chem.* **282**, 8641-8647.

13. Moradi, A., Hosseinkhani, S., Naderi-Manesh, H., Sadeghizadeh, M. and Alipour, B. S. (2009) Effect of charge distribution in a flexible loop on the bioluminescence color of Firefly luciferases. *Biochemistry* **48**, 575-582.

14. Alipour, B. S., Hosseinkhani, S., Ardestani, S. K. and Moradi, A. (2009) the effective role of positive charge saturation in bioluminescence color and thermostability of *firefly Luciferase*. *Photochem. Photobiol. Sci.* **8**, 847-855.

15. Arnold, K., Bordoli, L., Kopp, J. and Schwede, T. (2006) The Swiss-Model Workspace: a web-based environment for protein structure homology modelling. *Bioinformatics* **22**, 195-201.

16. Schwede, T., Kopp, J., Guex, N. and Peitsch, M. C. (2003) Swiss-Model: an automated protein homology-modeling server. *Nucleic. Acids. Res.* **31**, 3381-3385.

17. Guex, N. and Peitsch, M. C. (1997) Swiss-Model and the Swiss-PdbViewer: an environment for comparative protein modelling. *Electrophoresis* **18**, 2714-2723.

18. Conti, E., Franks, N. P. and Brick, P. (1996) Crystal structure of firefly luciferase throws light on a superfamily of adenylate-forming enzymes. *Structure* **4**, 287-298.

19. Myers, J. K., Pace, C. N. and Scholtz, M. (1995) Denaturant m-values and heat capacity changes: relation to changes in accessible surface areas of protein unfolding. *Protein Sci.* **4**, 2138-2148.

20. Roder, H. and Colon, W. (1997) Kinetic role of early intermediates in protein folding. *Curr. Opin. Struct. Biol.* **7**, 15-28.

21. Fersht, A. R., Matoushek, A. and Serrano, L. (1992) The folding of an enzyme. I. Theory of protein engineering analysis of stability and pathway of protein folding. *J. Mol. Biol.* **224**, 771-783.

22. Privalov, P. L. and Gill, S. J. (1988) Stability of protein structure and hydrophobic interaction. *Adv. Protein. Chem.* **39**, 191-263.

23. Privalov, P. L. and Gill, S. J. (1989) The Hydrophobic Effect, a Reappraisal. *Pure Appl. Chem.* **61**, 1907-1104.

24. Kuntz, I. D. (1971) Hydration of macromolecules. III Hydration of polypeptides. *J. Am. Chem. Soc.* **93**, 514-516.

25. Chiti, F., Stefani, M., Taddei, N., Ramponi, G. and Dobson, C. M. (2003) Rationalization of the effects of mutations on peptide and protein aggregation rates. *Nature* **424**, 805-808.

26. Pace, C. N. (1975) The stability of globular proteins. *CRC Crit. Rev. Biochem.* **3**, 1-43.

27. Pace, C. N. (1986) Determination and analysis of Urea and Guanidium Curves. *Methods Enzymol.* **131**, 266-279.

28. Zarrine-Afsar, A. and Davidson, A. R. (2004) The analysis of protein folding kinetic data produced in protein engineering experiments. *Methods* **34**, 41-50.

29. Eyring, H. (1935) the activated complex and the absolute rate of chemical reactions. *Chem. Rev.* **17**, 65-77.

30. Fersht, A. R., Matoushek, A., Bycroft, M., Kellis, J. T. and Serrano, L. (1991) Physical-organic molecular biology: pathway and stability of protein folding. *Pure Appl. Chem.* **63**, 187-194.